Materials Today: Proceedings xxx (xxxx) xxx

Contents lists available at ScienceDirect

Materials Today: Proceedings

journal homepage: www.elsevier.com/locate/matpr

Quantitative comparison between different methods for the determination of the amplified spontaneous emission threshold in dye-polymer blends and perovskite thin films

S. Milanese [a,*], M.L. De Giorgi [a], L. Cerdán [b], M.G. La-Placa [b], P.P. Boix [b], H.J. Bolink [b], M. Anni [a]

[a] Dipartimento di Matematica e Fisica "Ennio De Giorgi", Università del Salento, Via per Arnesano, 73100 Lecce, Italy
[b] Instituto de Ciencia Molecular, Universidad de Valencia, Paterna, Valencia 46980, Spain

ARTICLE INFO

Article history:
Available online xxxx

Keywords:
Amplified spontaneous emission
ASE threshold
Dye-polymer blend
Perovskite
Active waveguide

ABSTRACT

Amplified Spontaneous Emission (ASE) properties and ASE threshold are usually investigated for the characterization of a candidate active material for laser applications. However, the comparison among different materials is often hampered by the use in literature of several different methods to estimate the ASE threshold. In this work we quantitatively compare the ASE threshold values obtained by using the most employed methods in dye-doped polymer and lead halide perovskite thin films, highlighting the dependence of the value obtained on the applied method.

Selection and peer-review under responsibility of the scientific committee of the International Conferences & Exhibition on Nanotechnologies, Organic Electronics & Nanomedicine NANOTEXNOLOGY 2021.

1. Introduction

Since the discovery of stimulated optical radiation in 1960 [1] and the following demonstration of optical gain in organic dyes [2], laser applications have gained increasing attention in several areas, from scientific research up to medical application. Consequently, a great effort has been made to develop novel active materials for laser devices. Within this context, organic semiconductors stand out due to their low-cost processing techniques, chemical flexibility and optoelectronic properties tunability [3–5]. Among them, organic dyes have gained a central role in the scientific research and hundred of studies have been made to improve the operational stability of these small molecules embedded in polymeric matrices [4,5]. The demonstration of optical gain in both hybrid and fully inorganic perovskites [6,7] has then further broadened the horizons for the development of innovative active materials for solid state laser devices [8].

A typical experiment to demonstrate the presence of optical gain in a novel active material involves the study of the ASE properties of thin films acting as waveguides for the emitted photons, without the need of structures providing an optical feedback. In ASE, upon photo-excitation, the spontaneously emitted photons propagate along the active film, stimulating further emission and resulting in light amplification. In order to observe ASE, the Variable Pump Intensity (VPI) method is applied, in which the emission spectra are acquired as a function of the excitation density. Starting from low excitation values, the photoluminescence (PL) spectra of the sample initially show only spontaneous emission and, for high enough excitation density, ASE appears resulting in a lineshape variation, a spectral narrowing and a stronger increase of the output intensity.

In order to compare different active materials and choose the most suitable for a laser device, the ASE threshold is typically used as a parameter, and the material with its lowest value is thus considered the best one. Unfortunately, even if the sample to sample reproducibility of the ASE threshold is generally good in materials with good film forming properties [9,10], a quantitative comparison is often hindered by the ASE threshold dependence on the pump laser time length [6,11] and pump wavelength [12]. In addition, the lack of a unique definition of the ASE threshold and the presence of different experimental methods in the literature to determine it further complicates a meaningful comparison between different materials on the basis of their ASE threshold values. In particular, the most spread methods in the literature estimate the ASE threshold from the excitation density dependence of the output intensity: in an input–output intensity plot the threshold is found as the excitation density value corresponding

* Corresponding author.
E-mail address: stefania.milanese@unisalento.it (S. Milanese).

https://doi.org/10.1016/j.matpr.2022.04.656

Selection and peer-review under responsibility of the scientific committee of the International Conferences & Exhibition on Nanotechnologies, Organic Electronics & Nanomedicine NANOTEXNOLOGY 2021.

to a change of slope, which thus separates a regime in which the emission is dominated by the spontaneous emission and a regime in which ASE prevails [13–15].

Alternatively, the threshold can be estimated from the analysis of the spectral linewidth dependence on the excitation. In particular, as the ASE band is narrower than the spontaneous emission, one of the typical fingerprints of ASE is the spectral narrowing as it sets in and progressively dominates the emission. However, in this case there is no agreement on the method that has to be adopted to estimate the threshold: sometimes it is defined as the excitation density at which the Full Width at Half Maximum (FWHM) takes one half of the maximum value obtained from the spontaneous emission spectrum [16], sometimes as the excitation density corresponding to the beginning of the narrowing [17], in some cases the crossing of the best fit lines corresponding to the FWHM decrease [18] or, finally, the FWHM plot is considered just qualitatively. In addition to these, other ways to determine the ASE threshold can be found in literature, even if less spread, based on the excitation density dependence of the spectral lineshape [19] or on the estimate of the net gain of the material [20].

With the aim to understand how strongly the ASE threshold value depends on the methods used, a previous analysis was conducted [21] through the investigation of three polymeric active waveguides. In particular, the study evidenced that the FWHM was the quantity most sensitively affected by the presence of ASE and can provide the minimum threshold value by determining the beginning of the FWHM decrease (corresponding method being called "$FWHM_{narr}$"). However, the methods mainly used in the literature often take into account excitation densities at which the ASE is already a running and dominant process, rather than being at the beginning; for this reason, the corresponding values are systematically higher (up to 12 times) than the $FWHM_{narr}$ one.

In order to investigate the generality of these conclusions, in this work we extend the analysis to two other classes of active materials, namely dye-polymer blends and perovskites. In particular, we have analyzed a film of Rosamine4 embedded in a poly(2-hydroxyethyl methacrylate) (pHEMA) matrix [22] and a quasi-2D $BA_3MA_3Pb_5Br_{16}$ perovskite thin film [23].

Our analysis evidences that the best method to determine the beginning of the ASE is based on the visual determination of the lineshape variation as the excitation density increases. On the other side, the methods most used in the literature allow to determine the excitation regime in which ASE becomes the dominant emission process and provide values about 2.5 times higher than the visual threshold.

2. Materials and methods

Two samples have been chosen for our analysis: Rosamine4 in pHEMA as a dye-polymer sample [22] and a quasi-2D lead bromide $BA_3MA_3Pb_5Br_{16}$ perovskite thin film with emission spectra acquired at a temperature of 160 K [23]. The data analyzed in this work comes from the corresponding papers [22,23], that contain all the experimental details on the sample preparation and VPI measurements.

Both samples have been excited with a ns pulsed laser. In particular, Rosamine4 sample was optically pumped at 532 nm with 20 ns FWHM pulses from a frequency-doubled Q-switched Nd:YAG laser, operated at 5 Hz repetition rate; for the perovskite quasi-2D sample ASE properties have been explored by irradiating the films with a nitrogen laser at a wavelength of 337 nm delivering 3 ns pulses with a repetition rate of 20 Hz.

For each sample, the following eight methods have been applied to calculate the ASE threshold:

- Visual: it is the most rapid method to be applied since it only needs to visually observe the variation of the shape of the spectra at increasing excitation density and fix the threshold corresponding to the lowest excitation density allowing to observe an early-stage ASE
- FWHM/2: it considers the threshold as the excitation density value at which the FWHM becomes one half of the initial value obtained at low excitation density, when only spontaneous emission is present
- $FWHM_{aver}$: it fixes the ASE threshold as the excitation density value at which the FWHM reaches the average value between the maximum at low excitation density and the minimum at high excitation density
- $FWHM_{narr}$: it considers the beginning of the line narrowing as threshold; once defined the first point that deviates by more than one standard deviation from the initial constant fit line at low excitation density, the threshold is fixed as the average between this point and the one immediately before
- $FWHM_{cross}$: the ASE threshold comes from the crossing of the two best fit lines describing the trend of the FWHM as a function of the excitation density (knee of the curve, crossing of the constant and first decreasing fit lines)
- I_{TOT}: it plots the output intensity integrated over the spectral wavelength range as a function of the excitation density and fixes the threshold as the point of slope change
- I_{ASE}: it considers the excitation density dependence of the ASE contribution to the total integrated intensity and detects the threshold as the point of slope change
- I_{peak}: it plots the output intensity corresponding to the ASE peak wavelength and determines the ASE threshold as the point of slope change

3. Experimental results and discussion

3.1. Rosamine4

The PL spectra of Rosamine4 were acquired for excitation intensities from about 0.12 MW cm^{-2} to 4.2 MW cm^{-2}. For the sake of clarity, in Fig. 1a we only show some of them in order to evidence the dependence of the spectral lineshape as a function of the excitation intensity, near the threshold. We notice that at low pump intensities (below 0.6 MW cm^{-2}) the emission spectrum is characterized by a broad band peaked at about 580 nm with a shoulder at about 640 nm. Once the pump intensity reaches 0.62 MW cm^{-2}, a further shoulder starts to be visible and an ASE band becomes evident at about 600 nm for higher excitation intensities. The thicker orange line in Fig. 1a evidences the first pump intensity at which the PL spectrum begins to deviate from the spontaneous emission lineshape and represents the visual ASE threshold (0.62 MW cm^{-2}).

The analysis of the evolution of the spectral linewidth at increasing excitation intensity allowed to obtain the plot in Fig. 1b in which the FWHM is shown. At low pump values (below 0.6 MW cm^{-2}) the width of the PL spectra remains constant around 45 nm; then for higher excitation intensities (0.7 – 2.0 MW cm^{-2}) it suffers a narrowing and finally reaches a minimum plateau for higher pump intensity centered at about 10 nm, signaling that the ASE band is dominating the emission spectrum. Starting from the best fit curves, with a constant function at low and high excitation intensity and a linearly decreasing function in the narrowing excitation regime (red lines in Fig. 1b) and their one-standard-deviation uncertainty range (green lines in Fig. 1b), we determined the four ASE thresholds: $FWHM_{narr}$ = (0.720 ± 0.060) MW cm^{-2}; $FWHM_{cross}$ = (0.777 ± 0.058) MW cm^{-2}; FWHM/2 = (1.598 ± 0.053) MW cm^{-2} and $FWHM_{aver}$ = (1.389 ± 0.053) MW cm^{-2}.

The remaining ASE thresholds come from the analysis of the excitation intensity dependence of the output intensity. In Fig. 1c

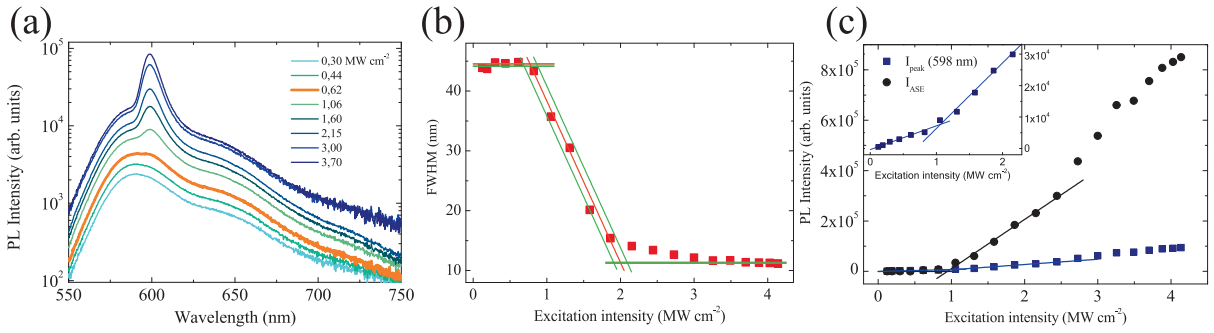

Fig. 1. (a) Excitation intensity dependence of PL spectra of the Rosamine4 sample. The thicker orange line evidences the first spectrum in which the lineshape is modified by the ASE presence. (b) Excitation intensity dependence of the PL spectra FWHM. The red lines represent the best fit curves and the green lines limit the uncertainty range. (c) Excitation intensity dependence of the ASE Integrated Intensity (black dots) and ASE peak Intensity (blue squares) with their relative best fit lines; inset: zoom of the I_{peak} plot focused on the slope change region. (For interpretation of the references to colour in this figure legend, the reader is referred to the web version of this article.)

the I_{ASE} and the I_{peak} plots with their respective best fit curves near the slope change regions are provided. The total integrated intensity dependence on the excitation intensity is not reported since the I_{TOT} plot lacks the typical inflection which allows the determination of the ASE threshold from the point of slope change. The calculated ASE thresholds are (0.946 ± 0.047) MW cm^{-2} and (1.062 ± 0.081) MW cm^{-2}, for the I_{ASE} and the I_{peak} intensity plots, respectively.

The results obtained from the application of all the methods are summarized in Table 1.

3.2. Quasi-2D BAMAPbBr perovskite

An analogous analysis has been performed on the perovskite thin film, whose ASE properties were tested at a temperature of 160 K. PL spectra are provided in Fig. 2a as a function of the excitation density, starting from a minimum value of 0.15 mJ cm^{-2} up to about 6 mJ cm^{-2}. The spontaneous emission is characterized by a broad band peaked at about 535 nm with a shoulder at about 520 nm; from 0.6 mJ cm^{-2} onwards (blue line highlighted in Fig. 2a) another emission band begins to be noticeable: it corresponds to the amplified radiation and will become a distinguished ASE peak centered at about 548 nm for higher excitation densities.

The FWHM for each spectrum has been determined and results are shown in Fig. 2b as a function of the excitation density. Here we can notice a small difference with respect to the dye sample: the linewidth indeed begins to decrease right from the lowest pump value (0–1 mJ cm^{-2}), before suffering a stronger narrowing at higher pump densities. Therefore, the lowest pump data have been fitted with a linear function (rather than a constant fit) and the $FWHM_{narr}$ threshold provided by the first point that deviates from this initial decreasing trend for more than one standard deviation was (1.14 ± 0.21) mJ cm^{-2}. The application of the other FWHM-based methods then gave the following ASE thresholds: $FWHM_{cross}$ = (0.788 ± 0.031) mJ cm^{-2}; FWHM/2 = (1.558 ± 0.014) mJ cm^{-2} and $FWHM_{aver}$ = (1.488 ± 0.014) mJ cm^{-2}. Looking at the excitation density dependence of the output intensity, we can notice a slope variation around (0.842 ± 0.053) mJ cm^{-2} and (1.165 ± 0.093) mJ cm^{-2} for the I_{ASE} and I_{peak} plots, respectively. ASE thresholds have been extracted from the intersection of the two best fit lines depicted in Fig. 2c. Also in this case the total integrated intensity plot is missing; the integrated output intensity does not show any slope variation since the spontaneous emission contribution remains important even at high excitation densities, covering the contribution of the stimulated radiation. All the results obtained for the perovskite sample are also summarized in Table 1.

The discussion on the method that has to be adopted to determine the ASE threshold results strictly related to the definition of the threshold itself. In our opinion two conditions are particularly meaningful:

- as the ASE is not present for too weak pumping, the ASE threshold could represent the minimum excitation density that allows to observe ASE in the spectra; in this perspective the experimental value closest to the real threshold is the minimum one
- from an applicative point of view, it is necessary to determine the excitation regime in which ASE is strong enough to dominate over the spontaneous emission; in this case the ASE threshold is related to a macroscopic variation of a feature of the total emission

The threshold values that we have obtained, in two very different active systems, interestingly show very similar dependence on the methods used (see Fig. 3a). In both cases the lowest values have been obtained from the application of the visual method, that can thus be considered the most reliable method to determine the beginning of the ASE. Moreover, the visual method is the only one that does not require any data analysis, but only the possibility to finely modify the pumping regime during the measurements.

Very similar results are also obtained for the methods based on the output intensity analysis. As already underlined, for both samples it was not possible to find a slope change from the total integrated intensity plot and therefore extract an ASE threshold through one of the methods most frequently used in literature. Moreover, the I_{peak} ASE threshold results higher than the I_{ASE} one in both cases, probably because the latter better isolates the ASE contribution of the emission in terms of integrated intensity, and it is not affected by the presence of the spontaneous emission.

Table 1
ASE threshold values obtained from the application of all methods for Rosamine4 and quasi-2D BAMAPbBr perovskite.

Method	ASE threshold	
	Rosamine4 (MW cm^{-2})	BAMAPbBr (mJ cm^{-2})
Visual	0.62	0.61
I_{TOT}	–	–
I_{ASE}	0.946 ± 0.047	0.842 ± 0.053
I_{peak}	1.062 ± 0.081	1.165 ± 0.093
$FWHM_{narr}$	0.720 ± 0.060	1.14 ± 0.21
$FWHM_{cross}$	0.777 ± 0.058	0.788 ± 0.031
$FWHM_{/2}$	1.598 ± 0.053	1.558 ± 0.014
$FWHM_{aver}$	1.389 ± 0.053	1.488 ± 0.014

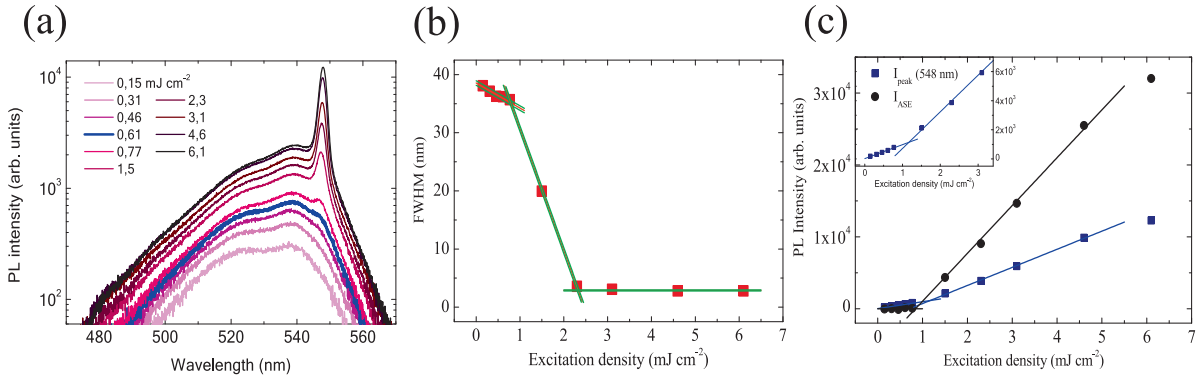

Fig. 2. (a) PL spectra of the quasi-2D BAMAPbBr sample at different excitation densities. Blue thicker line evidences the first spectrum at which ASE starts to be visible. (b) Plot of the linewidth (FWHM) as a function of the excitation density; red lines are the best fit curves, whereas green lines represent the uncertainty range. (c) Excitation density dependence of the ASE peak and integrated intensity (blue squares and black dots, respectively) with their relative best fit lines used for the determination of the ASE threshold; inset: zoom of the slope change for the I_{peak} plot. (For interpretation of the references to colour in this figure legend, the reader is referred to the web version of this article.)

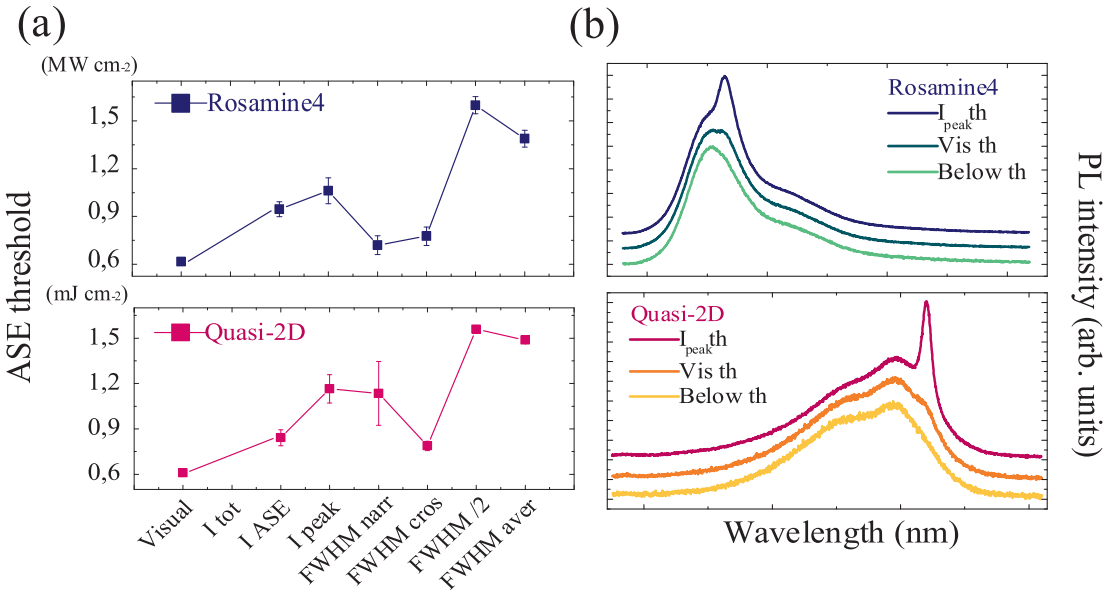

Fig. 3. (a) ASE threshold values obtained for Rosamine4 and quasi-2D perovskite as a function of the method used. (b) Comparison of PL spectra acquired at different excitation densities: at low pump value (Below threshold, "Below th"), near the lowest threshold ("Vis th") and in correspondence of the I_{peak} method threshold ("I_{peak} th"). The spectra are normalized to 1 at the spontaneous emission peak and vertically shifted for clarity.

Concerning the methods exploiting the FWHM dependence on the excitation regime, FWHM/2 is the most used one and, at the same time, is the method that provides the highest ASE threshold for both samples. However, once we exclude the visual analysis, the same FWHM plot allowed to extract the minimum ASE threshold too; for the Rosamine4 sample it is represented by the $FWHM_{cross}$ method, whereas for BAMAPbBr perovskite it is obtained from the application of the $FWHM_{narr}$ one.

In order to better evidence the different kind of information that is provided by the threshold values obtained with different methods, we compared the PL spectra acquired at different excitation densities (Fig. 3b); in particular, we considered pump values at which no ASE is present, one at the lowest threshold value (Visual threshold) and finally near the threshold obtained from one output intensity based method which is the most used in literature (I_{peak} threshold). The spectra clearly allow to observe that at the visual threshold excitation regime a small shoulder due to ASE is present, while close to the I_{peak} threshold the ASE band is clearly visible.

4. Conclusion

In this work we have analyzed the ASE properties of a film of Rosamine4 in pHEMA matrix and a quasi-2D $BA_3MA_3Pb_5Br_{16}$ perovskite thin film. For each sample, the excitation density dependence of different spectral features has been studied and the ASE threshold has been calculated through the methods most spread in the literature, for a total number of eight methods.

The results evidence that the beginning of the ASE process is better detected by the Visual method, which exploits the excitation density dependence of the spectral lineshape and provides the lowest ASE threshold values for both samples.

On the other hand, excitation regimes in which ASE is a dominant process are well described either from methods based on the slope change (such as I_{peak} and I_{ASE}), or from the ones which are based on the FWHM variation (FWHM/2 and the less spread $FWHM_{aver}$, in particular). However, it has been observed that for both samples the output intensity based methods provide ASE

thresholds smaller than those based on the spectral linewidth analysis. As a consequence, in this instance the former can be chosen to identify an excitation regime of ASE dominance (I_{peak} method, for example).

CRediT authorship contribution statement

S. Milanese: Conceptualization, Methodology, Formal analysis, Investigation, Data curation, Writing – original draft. **M.L. De Giorgi:** Conceptualization, Methodology, Writing – review & editing. **L. Cerdán:** Conceptualization, Resources, Writing – review & editing. **M.G. La-Placa:** Conceptualization, Resources, Writing – review & editing. **P.P. Boix:** Conceptualization, Resources, Writing – review & editing. **H.J. Bolink:** Conceptualization, Resources, Writing – review & editing. **M. Anni:** Conceptualization, Methodology, Writing – review & editing, Visualization, Supervision.

Declaration of Competing Interest

The authors declare that they have no known competing financial interests or personal relationships that could have appeared to influence the work reported in this paper.

References

[1] T.H. Maiman, Stimulated Optical Radiation in Ruby, Nature 187 (4736) (1960) 493–494, https://doi.org/10.1038/187493a0.
[2] F.P. Schäfer, W. Schmidt, J. Volze, Organic Dye Solution Laser, Appl. Phys. Lett. 9 (8) (1966) 306–309, https://doi.org/10.1063/1.1754762.
[3] C. Grivas, M. Pollnau, Organic solid-state integrated amplifiers and lasers, Laser Photon. Rev. 6 (2012) 419–462, https://doi.org/10.1002/lpor.201100034.
[4] A.J.C. Kuehne, M.C. Gather, Organic Lasers: Recent Developments on Materials, Device Geometries and Fabrication Techniques, Chem. Rev. 116 (21) (2016) 12823–12864, https://doi.org/10.1021/acs.chemrev.6b00172.
[5] M. Anni, S. Lattante, Organic Lasers: Fundamentals, Developments, and Applications, Jenny Stanford Publishing (2018).
[6] S. Yakunin, L. Protesescu, F. Krieg, M.I. Bodnarchuk, G. Nedelcu, M. Humer, G. De Luca, M. Fiebig, W. Heiss, M.V. Kovalenko, Low-threshold Amplified Spontaneous Emission and Lasing from Colloidal Nanocrystals of Caesium Lead Halide Perovskites, Nat. Commun. 6 (2015) 8515, https://doi.org/10.1038/ncomms9515.
[7] Z. Liu, Z. Hu, Z. Zhang, J. Du, J. Yang, X. Tang, W. Liu, Y. Leng, Two-Photon Pumped Amplified Spontaneous Emission and Lasing from Formamidinium Lead Bromine Nanocrystals, ACS Photon. 6 (12) (2019) 3150–3158, https://doi.org/10.1021/acsphotonics.9b01226.
[8] M.L. De Giorgi, M. Anni, Amplified Spontaneous Emission and Lasing in Lead Halide Perovskites: State of Art and Perspectives, Appl. Sci. 9 (21) (2019) 4591, https://doi.org/10.3390/app9214591.
[9] M. Anni, The role of the β-phase content on the stimulated emission of poly (9,9-dioctylfluorene) thin films, Appl. Phys. Lett. 93 (2) (2008) 023308, https://doi.org/10.1063/1.2957669.
[10] M. Anni, M. Alemanno, Temperature dependence of the amplified spontaneous emission of poly(9,9-dioctylfluorene) β phase, Phys. Rev. B 78 (2008) 233102, https://doi.org/10.1103/PhysRevB.78.233102.
[11] Z.E. Lampert, S.E. Lappi, J.M. Papanikolas, C. Lewis Reynolds Jr., Intrinsic optical gain in thin films of a conjugated polymer under picosecond excitation, Appl. Phys. Lett. 103 (2013) 033303, https://doi.org/10.1063/1.4816040.
[12] S.M.H. Qaid, H.M. Ghaithan, K.K. AlHarbi, A.F.B. Ajaj, B.A. Al-Asbahi, A.S. Aldwayyan, Investigation of Threshold Carrier Densities in the Optically Pumped Amplified Spontaneous Emission of Formamidinium Lead Bromide Perovskite Using Different Excitation Wavelengths, Photonics 9 (2022) 4, https://doi.org/10.3390/photonics9010004.
[13] R. Muñoz-Mármol, P.G. Boj, J.M. Villalvilla, J.A. Quintana, N. Zink-Lorre, Á. Sastre-Santos, J. Aragó, E. Ortí, P. Baronas, D. Litvinas, S. Juršėnas, F. Fenández-Lázaro, M.A. Díaz-García, Effect of Substituents at Imide Positions on the Laser Performance of 1,7-Bay-Substituted Perylenediimide Dyes, J. Phys. Chem. C 125 (22) (2021) 12277–12288, https://doi.org/10.1021/acs.jpcc.1c00833.
[14] L.u. Zhang, J. Wen, X. Ren, S. Jin, S. Liu, Synergistically Enhanced Amplified Spontaneous Emission by Cd Doping and Cl-Assisted Crystallization, Adv. Opt. Mater. 9 (4) (2021) 2001825, https://doi.org/10.1002/adom.202001825.
[15] M.L. De Giorgi, T. Lippolis, N.F. Jamaludin, C. Soci, A. Bruno, M. Anni, Origin of Amplified Spontaneous Emission Degradation in MAPbBr 3 Thin Films under Nanosecond-UV Laser Irradiation, J. Phys. Chem. C 124 (19) (2020) 10696–10704, https://doi.org/10.1021/acs.jpcc.0c02331.
[16] V. Bonal, M. Morales-Vidal, P.G. Boj, J.M. Villalvilla, J.A. Quintana, N. Lin, S. Watanabe, H. Tsuji, E. Nakamura, M.A. Díaz-García, Kinetically Protected Carbon-Bridged Oligo(p-phenylenevinylene) Derivatives for Blue Color Amplified Spontaneous Emission, Bull. Chem. Soc. Jpn. 93 (6) (2020) 751–758, https://doi.org/10.1246/bcsj.20200042.
[17] C. Kallinger, S. Riechel, O. Holderer, U. Lemmer, J. Feldmann, S. Berleb, A.G. Muckl, W. Brutting, Picosecond Amplified Spontaneous Emission Burst from a Molecularly Doped Organic Semiconductor, J. Appl. Phys. 91 (2002) 6367–6370, https://doi.org/10.1063/1.1466879.
[18] M.L. De Giorgi, A. Perulli, N. Yantara, P.P. Boix, M. Anni, Amplified Spontaneous Emission Properties of Solution Processed $CsPbBr_3$ Perovskite Thin Films, J. Phys. Chem. C 121 (27) (2017) 14772–14778, https://doi.org/10.1021/acs.jpcc.7b00854.
[19] A.O. Murzin, B.V. Stroganov, C. Günnemann, S.B. Hammouda, A.V. Shurukhina, M.S. Lozhkin, A.V. Emeline, Y.V. Kapitonov, Amplified Spontaneous Emission and Random Lasing in $MAPbBr_3$ Halide Perovskite Single Crystals, Adv. Opt. Mater. 8 (17) (2020) 2000690, https://doi.org/10.1002/adom.202000690.
[20] L. Cerdán, A. Costela, I. García-Moreno, O. García, R. Sastre, Waveguides and quasi-waveguides based on pyrromethene 597-doped poly(methyl methacrylate), Appl. Phys. B 97 (1) (2009) 73–83, https://doi.org/10.1007/s00340-009-3518-8.
[21] S. Milanese, M.L. De Giorgi, M. Anni, Determination of the Best Empiric Method to Quantify the Amplified Spontaneous Emission Threshold in Polymeric Active Waveguides, Molecules 25 (13) (2020) 2992, https://doi.org/10.3390/molecules25132992.
[22] L. Cerdán, V. Martínez-Martínez, I. García-Moreno, A. Costela, M.E. Pérez-Ojeda, I.L. Arbeloa, L. Wu, K. Burgess, Naturally Assembled Excimers in Xanthenes as Singular and Highly Efficient Laser Dyes in Liquid and Solid Media, Adv. Opt. Mater. 1 (12) (2013) 984–990, https://doi.org/10.1002/adom.201300383.
[23] M.L. De Giorgi, A. Cretì, M.G. La-Placa, P.P. Boix, H.J. Bolink, M. Lomascolo, M. Anni, Amplified Spontaneous Emission in Thin Film of Quasi-2D $BA_3MA_3Pb_5Br_{16}$ Lead Halide Perovskites, Nanoscale 13 (2021) 8893–8900, https://doi.org/10.1039/D0NR08799H.